*Inorg. Chem.* **2006**, *45*, 5630–5634


# Stabilization of a Monomethyl Orthomolybdate in the Binding Pocket of a Dinuclear Cobalt Complex

**Vasile Lozan and Berthold Kersting***

*Institut für Anorganische Chemie, Universität Leipzig, Johannisallee 29, 04103 Leipzig, Germany*

Received March 6, 2006

The ability of the dinuclear $Co^{II}$ complex $[(L^{Me})Co^{II}_2(\mu\text{-Cl})]^+$ [**1**; $(L^{Me})^{2-}$ = 3,6,9,17,20,23-hexamethyl-3,6,9,17,20,-23-hexaaza-29,30-dithiol-13,27-di-*tert*-butyltricyclo[23.3.1$^{11.15}$]triaconta-1(28),11,13,15(30),25,26-hexaene] to bind tetrahedral oxoanions of the transition metal has been investigated. Two new complexes, $[(L^{Me})Co^{II}_2(\mu\text{-}MoO_4)]$ (**2**) and $[(L^{Me})Co^{II}_2(\mu\text{-}MoO_3(OMe))]_2[Mo_4O_{10}(OMe)_6]$ (**3**), were prepared by substitution reactions of **1** with $(n\text{-}Bu_4N)_2\text{-}MoO_4$ in MeCN or with $MoO_3{\cdot}2H_2O/NEt_3$ in MeOH. Both compounds were characterized by X-ray crystallography. The dioctahedral complex **2** features a $\mu_{1,3}$-bridging $MoO_4^{2-}$ unit, whereas the cation in **3** hosts an unprecedented $\mu_{1,3}\text{-}MoO_3(OMe)^-$ motif, demonstrating that four-coordinate molybdate esters can be stabilized in the binding pocket of the bowl-shaped $[(L^{Me})Co^{II}_2]^{2+}$ complex. The results of IR, UV/vis, and cyclic voltammetry measurements are also reported.

## Introduction

The synthesis and structural characterization of a large number of polynuclear oxo−alkoxo species of hexavalent Mo have been reported. Typical examples are polymeric $[Mo_2O_5(OMe)_2]$,[1] tetranuclear $[Mo_4O_{10}(OMe)_6]^{2-}$,[2] and octanuclear $[Mo_8O_{24}(OMe)_4]^{4-}$,[3] which can be readily prepared by solvolysis reactions of soluble isopolymolybdate anion precursors, such as $(n\text{-}Bu_4N)_2[Mo_2O_7]$ and $(n\text{-}Bu_4N)_4\text{-}[Mo_8O_{28}]$, in methanol.[4] While the coordination chemistry of the polynuclear oxo−alkoxo molybdates is now fairly well-understood,[5] surprisingly little is known about their monomeric $Mo^{VI}O_x(OR)_y$ congeners. In particular, four-coordinate molybdenum oxoalkoxides are difficult to stabilize. The neutral alkyl esters, $MoO_2(OR)_2$, bearing primary alkoxy groups (R = Me, Et, Pr) are Lewis acidic[6] and tend to oligomerize in the solution as well as in the solid state.[7] Monomeric, four-coordinate species, such as $MoO_2(O\text{-}t\text{-}Bu)_2$,[8] $MoO_2(OSiPh_3)_2$,[9] and $MoO_2(O\text{-}2,6\text{-}t\text{-}Bu_2C_6H_3)_2$,[10] are only accessible with bulky alkoxides. The same is true for the anionic $MoO_3(OR)^-$ compounds. Stable species, such as $[MoO_3(OSi\text{-}t\text{-}Bu_3)]^-$,[11] do exist but only with bulky ligands.[12,13] We now demonstrate that the parent $MoO_3(OCH_3)^-$ complex can be stabilized by the steric protection of the supporting ligand $(L^{Me})^{2-}$ in the dinuclear Co complex $[(L^{Me})Co_2]^{2+}$ [14] (Chart 1).

Our study was initiated by the finding that tetrahedral oxoanions, such as $ClO_4^-$,[15] $H_2PO_4^-$,[16] and $H_2PO_2^-$,[17] can be readily accommodated in the binding pocket of the dinuclear $[(L^{Me})M_2]^{2+}$ complexes (Chart 1). This led us to study the ability of the $[(L^{Me})M_2]^{2+}$ fragment to bind tetrahedral oxoanions of the transition metals.[18] In the course of our studies, we have been able to trap the elusive $MoO_3(OMe)^-$ ion. Herein, we report on these findings.

* To whom correspondence should be addressed. E-mail: b.kersting@uni-leipzig.de.

(1) McCarron, E. M.; Staley, R. H.; Sleight, A. W. *Inorg. Chem.* **1984**, *23*, 1043−1045.
(2) Liu, S.; Shaikh, S. N.; Zubieta, J. *Inorg. Chem.* **1987**, *26*, 4303−4305.
(3) McCarron, E. M.; Harlow, R. L. *J. Am. Chem. Soc.* **1983**, *105*, 6179−6181.
(4) Liu, S.; Shaikh, S. N.; Zubieta, J. *Inorg. Chem.* **1989**, *28*, 723−732.
(5) Kang, H.; Liu, S.; Shaikh, S. N.; Nicholson, T.; Zubieta, J. *Inorg. Chem.* **1989**, *28*, 920−933.
(6) Piarulli, U.; Williams, D. N.; Floriani, C.; Gervasio, G.; Viterbo, D. *J. Chem. Soc., Dalton Trans.* **1995**, 3329−3334.
(7) Kim, G. S.; Huffman, D.; DeKock, C. W. *Inorg. Chem.* **1989**, *28*, 1279−1283.
(8) Chisholm, M. H.; Folting, K.; Huffman, J. C.; Kirkpatrick, C. C. *Inorg. Chem.* **1984**, *23*, 1021−1037.
(9) Huang, M.; DeKock, C. W. *Inorg. Chem.* **1993**, *32*, 2287−2291.
(10) Hanna, T. A.; Incarvito, C. D.; Rheingold, A. L. *Inorg. Chem.* **2000**, *39*, 630−631.
(11) Klemperer, W. G.; Mainz, V. V.; Shum, W.; Wang, R. C. *Inorg. Chem.* **1985**, *24*, 1968−1970.
(12) Lubben, T. V.; Wolczanski, P. T.; Van Duyne, G. D. *Organometallics* **1984**, *3*, 977−983.
(13) Hvoslef, J.; Hope, H.; Murray, B. D.; Power, P. P. *Chem. Commun.* **1983**, 1438−1439.
(14) Steinfeld, G.; Kersting, B. *Inorg. Chem.* **2002**, *41*, 1140−1150.
(15) Yournaux, Y.; Lozan, V.; Klingele, J.; Kersting, B. *Chem. Commun.* **2006**, 83−84.
(16) Kersting, B. *Angew. Chem.* **2001**, *113*, 4110−4112; *Angew. Chem., Int. Ed.* **2001**, *40*, 3988−3990.
(17) Kersting, B.; Steinfeld, G.; Lozan, V. Unpublished results.
(18) McKee, V.; Nelson, J.; Town, R. M. *Chem. Soc. Rev.* **2003**, *32*, 309−325.



10.1021/ic0603656 CCC: $33.50 
Published on Web 05/25/2006

**Chart 1.** Coordination Mode of $(L^{Me})^{2-}$ in Complexes of the Type $[(L^{Me})M_2(\mu\text{-}L')]^+$ and Schematic Representation of Their Bowl-Shaped Structures (L′ = Coligand)

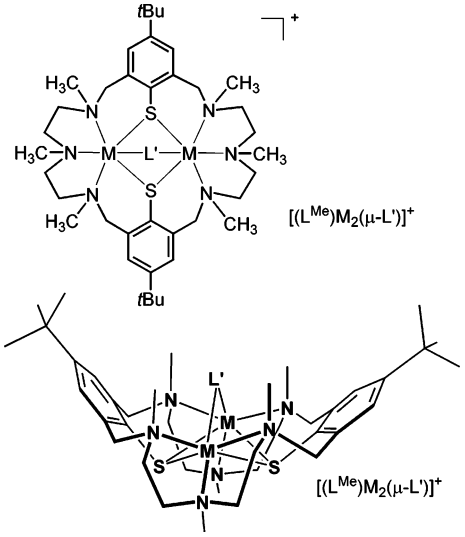


## Experimental Section

**Materials and Methods.** All preparations were carried out under a protective atmosphere of argon. Reagent-grade solvents were used throughout. $[(L^{Me})Co_2(\mu\text{-Cl})]ClO_4$ (**1**) was prepared as previously described.[16] $(n\text{-}Bu_4N)_2MoO_4$ was prepared from $MoO_3{\cdot}2H_2O$[19] and $(n\text{-}Bu_4N)OH$ following the procedure used for the preparation of $(n\text{-}Bu_4N)_2WO_4$.[20] All other reagents were obtained from standard commercial sources and used without further purifications. Melting points were determined in open glass capillaries and are uncorrected. IR spectra were recorded on a Bruker VECTOR 22 Fourier transform infrared spectrometer. The electronic absorption spectra were measured on a Jasco V-570 UV/vis/NIR spectrometer. Elemental analyses were carried out with a Vario EL elemental analyzer. Electrochemical measurements were performed as previously described.[14] Cobaltocenium hexafluorophosphate ($CoCp_2PF_6$) was used as an internal standard. All potentials were converted to the saturated calomel electrode (SCE) reference using tabulated values.[21]

***Caution!*** *Perchlorate salts are potentially explosive and should therefore be prepared only in small quantities and handled with appropriate care.*

**$[(L^{Me})Co_2(\mu\text{-}MoO_4)]$ (2).** To a solution of $[(L^{Me})Co_2(\mu\text{-Cl})]ClO_4$ (184 mg, 0.200 mmol) in acetonitrile (40 mL) was added $(n\text{-}Bu_4N)_2MoO_4$ (258 mg, 0.400 mmol) in acetonitrile (5 mL). The green-blue reaction mixture was stirred for 12 h. The resulting brown-red precipitate was filtered, washed with cold methanol, and dried in air. The crude product was purified by recrystallization from dichloromethane/ethanol. Yield: 165 mg (84%). Mp: 338−339 °C (dec). IR (KBr disk): $\tilde{\nu}$ 3421(s), 3047(vw), 2963(s), 2950(s), 2900(m), 2865(s), 2835(m), 2800(w), 1641(m), 1477(sh), 1458(vs), 1421(m), 1393(m), 1362(m), 1348(w), 1324(w), 1305(w), 1292(sh), 1261(m), 1230(m), 1204(m), 1170(w), 1154(m), 1130(w), 1114(w), 1079(s), 1060(s), 1046(s), 1003(m), 982(w), 928(m), 911(m), 880(m), 861(vs), 849(vs), 822(vs), 807(vs), 753(m), 626(m) $cm^{-1}$. UV/vis ($CH_2Cl_2$): 434 (370), 508 (114), 550 (144), 571 (136), 624 (51), 703 (28), 1307 nm (54 $M^{-1}$ $cm^{-1}$). Elem anal. Calcd for $C_{38}H_{64}Co_2MoN_6O_4S_2{\cdot}2H_2O$ (946.89 + 36.03): C, 46.43; H, 6.97; N, 8.55; S, 6.52. Found: C, 46.12; H, 7.27; N, 8.23; S, 6.20.

**$[(L^{Me})Co^{II}_2(\mu\text{-}MoO_3(OMe))]_2[Mo_4O_{10}(OMe)_6]$ (3).** To a suspension of $MoO_3(H_2O)_2$ (90 mg, 0.50 mmol) in methanol (40 mL) was added a solution of $NEt_3$ (101 mg, 1.00 mmol) in methanol (1 mL). To the resulting clear solution was added solid $[(L^{Me})Co_2(\mu\text{-Cl})]ClO_4$ (184 mg, 0.200 mmol), and the reaction mixture was stirred for 12 h at ambient temperature. The resulting brown-red microcrystalline solid was isolated by filtration, washed with a few milliliters of methanol, and dried in air. Yield: 126 mg (0.047 mmol, 47% based on **1**). Mp: >365 °C (dec). IR (KBr disk): $\tilde{\nu}$ 3445(s), 3044(vw), 2963(sh), 2953(s), 2902(m), 2868(s), 2837(sh), 2808(w), 1637(br), 1478(sh), 1460(vs), 1424(m), 1394(m), 1363(m), 1350(w), 1338(w), 1305(m), 1291(sh), 1264(m), 1231(m), 1201(m), 1167(w), 1152(m), 1132(w), 1111(w), 1075(s), 1059(s), 1043(s), 1000(m), 981(w), 941(s), 912(s), 880(s), 819(vs), 804(vs), 754(s), 706(s), 678(s), 628(w) $cm^{-1}$. Elem anal. Calcd for $C_{84}H_{152}Co_4Mo_6N_{12}O_{24}S_4{\cdot}6H_2O$ (2653.8 + 108.09): C, 36.53; H, 5.99; N, 6.09; S, 4.64. Found: C, 35.95; H, 5.62; N, 6.37; S, 4.61.

**X-ray Crystallography.** Crystals of **2**·$CH_2Cl_2$ were obtained from dichloromethane. Crystals of **3**·6MeOH were picked from the filtrate of the reaction mixture. Crystal data and collection details are reported in Table 1. The diffraction experiments were carried out at 210(2) K on a Bruker CCD X-ray diffractometer using Mo Kα radiation. The data were processed with *SAINT*[22] and corrected for absorption using *SADABS*.[23] Structures were solved by direct methods and refined by full-matrix least-squares with *SHELXL-97* on the basis of all data using $F^2$.[24] H atoms were placed in calculated positions and treated isotropically using the 1.2-fold $U_{iso}$ value of the parent atom except methyl protons, which were assigned the 1.5-fold $U_{iso}$ value of the parent C atoms. All non-H atoms, except the O and C atoms of the MeOH solvates in **3**·6MeOH, were refined anisotropically. In the crystal structure of **3**·6MeOH, one *t*-Bu group was found to be disordered over two positions. The two orientations were refined by using the SADI instruction (equal C−C and C···C distances, respectively) implemented in the *ShelXL* program to give site occupancies of 0.74(1) (for C36a−C18a) and 0.26(1) (for C36b−C38b). The 10 largest residual peaks (0.97−0.70 $e^-/Å^3$) in the final Fourier map of **3**·

**Table 1.** Crystallographic Data for **2**·$CH_2Cl_2$ and **3**·$6CH_3OH$

| param | **2**·$CH_2Cl_2$ | **3**·$6CH_3OH$ |
|---|---|---|
| formula | $C_{39}H_{66}Cl_2Co_2MoN_6O_4S_2$ | $C_{90}H_{176}Co_4Mo_6N_{12}O_{30}S_4$ |
| fw | 1031.80 | 2846.03 |
| space group | $P2_1/n$ | $P\bar{1}$ |
| $a$ (Å) | 14.214(3) | 14.229(3) |
| $b$ (Å) | 18.257(4) | 14.514(3) |
| $c$ (Å) | 18.259(4) | 16.862(3) |
| α (deg) | 90.00 | 65.34(3) |
| $\beta$ (deg) | 108.32(3) | 70.77(3) |
| $\gamma$ (deg) | 90.00 | 75.23(3) |
| $V$ (Å$^3$) | 4498.1(17) | 2960.0(10) |
| $Z$ | 4 | 1 |
| $D_{calc}$ (g/cm$^3$) | 1.524 | 1.597 |
| $\mu$ (mm$^{-1}$) | 1.261 | 1.301 |
| R1[a] (R1 all data) | 0.0785 (0.2053) | 0.0527 (0.1222) |
| wR2[b] (wR2 all data) | 0.1852 (0.2468) | 0.1146 (0.1391) |

[a] $R1 = \sum||F_o| - |F_c||/\sum|F_o|$. [b] $wR2 = \{\sum[w(F_o^2 - F_c^2)^2]/\sum[w(F_o^2)^2]\}^{1/2}$.

(19) Brauer, G. *Handbuch der Präparativen Anorganischen Chemie*, 3rd ed.; Ferdinand Enke Verlag: Stuttgart, Germany, 1981; p 1544.
(20) Clegg, W.; Errington, R. J.; Fraser, K. A.; Richards, D. G. *J. Chem. Soc., Chem. Commun.* **1993**, 1105−1107.
(21) Connelly, N. G.; Geiger, W. E. *Chem. Rev.* **1996**, *96*, 877−910. Under our experimental conditions, $E(Cp_2Co^+/Cp_2Co) = -1.345$ V vs $E(Cp_2Fe^+/Cp_2Fe)$; $E(Cp_2Co^+/Cp_2Co) = -0.937$ V vs SCE.
(22) *SAINT*+, version 6.02; Bruker AXS: Madison, WI, 1999.
(23) Sheldrick, G. M. *SADABS, Area-Detector Absorption Correction*; University of Göttingen: Göttingen, Germany, 1996.
(24) Sheldrick, G. M. *SHELXL-97, Computer program for crystal structure refinement*; University of Göttingen: Göttingen, Germany, 1997.

**Scheme 1.** Synthesis of Complexes **2** and **3**

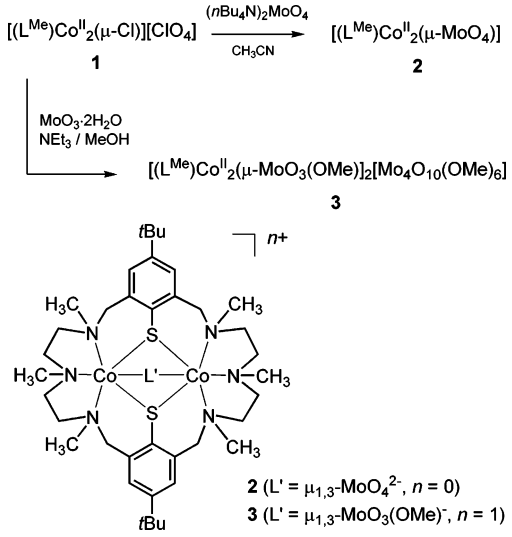


6MeOH are located in the vicinity of the Mo atoms of the $[Mo_4O_{10}(OMe)_6]^{2-}$ anion [Q2, Q5, Q7; $d$(Mo···Q) < 0.95 Å], the S and Co atoms of the cation [Q1, Q8, Q9, Q10; $d$(S···Q1,Co···Q) < 1.29 Å], and the MeOH solvates [Q3, Q4, Q6; $d$(C···Q) < 1.12 Å]. The highest residual peak around the $MoO_3(OMe)^-$ ion (Q17 = 0.66 e$^-$/Å$^3$) is at a distance of 1.19 Å from the Mo atom. The one large residual peak for **2** is associated with the $CH_2Cl_2$ molecule (Q1···Cl1 = 0.10 Å). The electron density map is otherwise featureless.

## Results and Discussion

**Synthesis and Characterization of Compounds.** The neutral $Co^{II}_2$ complex **2** was chosen as the target compound. Following the method of preparation of $[(L^{Me})Ni_2(O_2P(OH)_2)]^+$ from $[(L^{Me})Ni_2(Cl)]^+$ and $(n\text{-}Bu_4N)H_2PO_4$,[16] **1** was treated with $(n\text{-}Bu_4N)_2MoO_4$,[19,20] in $CH_3CN$ at ambient temperature for 12 h, as indicated in Scheme 1, to yield **2** as a pale-red powder. Recrystallization from dichloromethane/ethanol produced analytically pure material in 84% yield.

In another attempt, we tried to synthesize **2** by the direct reaction of **1** with an excess of $(HNEt_3)_2MoO_4$ (prepared in situ from $MoO_3{\cdot}2H_2O$ and $NEt_3$)[25,26] in methanol, but this resulted in the formation of **3**, which was reproducibly obtained as a dark-red-brown microcrystalline solid in ca. 45% yield. Attempts to generate a similar product by methanolysis of **1** have failed. Thus, the formation of **3** is simply a matter of trapping this species from solution. All compounds gave satisfactory elemental analyses and were characterized by spectroscopic methods (IR and UV/vis), cyclic voltammetry, and X-ray crystallography.

The IR spectrum of **2** in KBr shows three strong absorptions at 861, 848, and 807 cm$^{-1}$, which are tentatively assigned to the $\nu_1(A_1)$ and $\nu_3(F_2)$ stretching modes of the $MoO_4^{2-}$ unit.[27] The splitting of $\nu_3$ can be traced back to the lower local symmetry of the $\eta^2$-bonded $MoO_4^{2-}$ ion (see the crystal structure described below). The IR spectrum of **3** exhibits several absorbances in the 950−678-cm$^{-1}$ region.

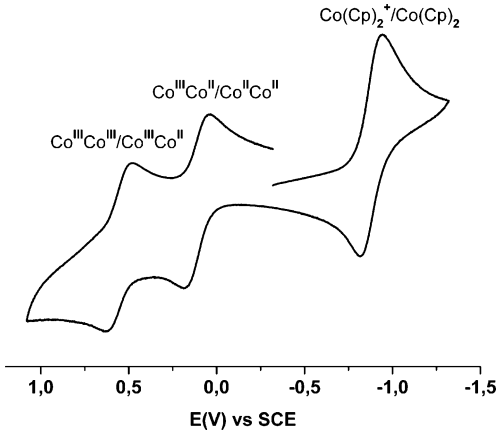


**Figure 1.** Cyclic voltammogram of **2** in dichloromethane at 295 K. Experimental conditions: 0.1 M $[n\text{-}Bu_4N][PF_6]$, ca. $1 \times 10^{-3}$ M sample concentration, Pt disk working electrode, Ag wire reference electrode, scan rate 100 mV/s, $[Co(Cp)_2]PF_6$ internal reference.

The bands at 941, 913, 880, 751, and 678 cm$^{-1}$ can be assigned to the various Mo−O stretching frequencies of the $[Mo_4O_{10}(OMe)_6]^{2-}$ anion. Similar values have been reported for $[Ph_3MeP]_2[Mo_4O_{10}(OCH_3)_6]$.[5] The two remaining absorptions at 803 and 818 cm$^{-1}$ can then be attributed to the Mo−O stretching modes of the $[MoO_3(OCH_3)]^-$ unit, but these values should be taken as indicative rather than definitive. There may be further bands associated with the coligand that are obscured by the $[Mo_4O_{10}(OMe)_6]^{2-}$ absorptions. The UV/vis spectrum of **2** is very similar to that of **1**, displaying typical weak d−d transitions of octahedral high-spin $Co^{II}$ in the 300−1600-nm range.[28] The weak broad band at 1307 nm can be assigned to the $^4T_{1g}(F) \rightarrow {}^4T_{2g}$ transition. The features in the 500−630-nm region are attributable to components of the parent octahedral $^4T_{1g}(F) \rightarrow {}^4T_{1g}(P)$ and $^4T_{1g}(F) \rightarrow {}^4A_{2g}$ ligand field transitions split by lower symmetry.

In view of the air stability of **2**, it was of interest to determine its redox properties. Figure 1 shows its cyclic voltammogram in a dichloromethane solution. Two waves, one at $E^1_{1/2} = +0.10$ V (vs SCE) with a peak-to-peak separation of 140 mV and one at $E^2_{1/2} = +0.55$ V with a peak-to-peak separation of 146 mV, are observed. These oxidations correspond to metal-centered oxidations of the $Co^{II}Co^{II}$ species **2** to its mixed-valent $Co^{II}Co^{III}$ and fully oxidized $Co^{III}Co^{III}$ forms (eqs 1 and 2, respectively). Thus, as was observed previously for **1**, the divalent $Co^{II}$ oxidation level is enormously stabilized over the trivalent state. Likewise, within our potential window, no reductions of the $MoO_4^{2-}$ ion are detected.

$$[(L^{Me})Co^{III}Co^{II}(MoO_4)]^+ + e^- \leftrightarrow [(L^{Me})Co^{II}_2(MoO_4)] \qquad E^1_{1/2} \quad (1)$$

$$[(L^{Me})Co^{III}Co^{III}(MoO_4)]^{2+} + e^- \leftrightarrow [(L^{Me})Co^{III}Co^{II}(MoO_4)]^+ \qquad E^2_{1/2} \quad (2)$$

(25) Fuchs, J. *Z. Naturforsch.* **1973**, *28b*, 389−404.
(26) Thiele, A.; Fuchs, J. *Z. Naturforsch.* **1979**, *34b*, 145−154.
(27) Coomber, R.; Griffith, W. P. *J. Chem. Soc. A* **1968**, 1128−1131.
(28) Journaux, Y.; Glaser, T.; Steinfeld, G.; Lozan, V.; Kersting, B. *J. Chem. Soc., Dalton Trans.* **2006**, 1738−1748.

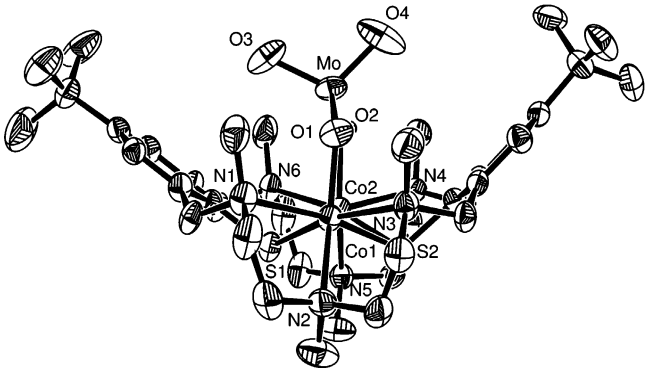


**Figure 2.** Structure of the neutral complex **2** in crystals of **2**·$CH_2Cl_2$. Thermal ellipsoids are drawn at the 50% probability level. H atoms are omitted for reasons of clarity. Selected bond lengths [Å] and angles [deg]: Mo−O(1) 1.756(6), Mo−O(2) 1.765(6), Mo−O(3) 1.714(7), Mo−O(4) 1.710(7), Co(1)−O(1) 1.988(6), Co(2)−O(2) 1.988(6), Co(1)−N(1) 2.312(7), Co(1)−N(2) 2.227(7), Co(1)−N(3) 2.322(7), Co(1)−S(1) 2.526(3), Co(1)−S(2) 2.521(3), Co(2)−N(4) 2.324(7), Co(2)−N(5) 2.219(7), Co(2)−N(6) 2.320(7), Co(2)−S(1) 2.498(2), Co(2)−S(2) 2.554(2); O−Mo−O 106.3(3)−111.5(3)°.

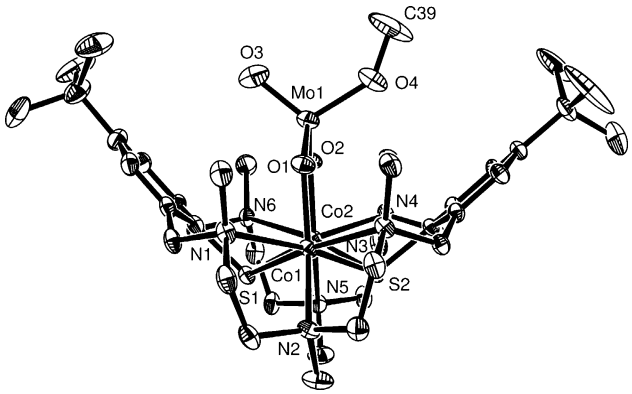


**Figure 3.** Structure of the $[(L^{Me})Co^{II}_2(MoO_3(OCH_3))]^+$ cation in crystals of **3**·6$CH_3OH$. Thermal ellipsoids are drawn at the 50% probability level. H atoms are omitted for reasons of clarity. Selected bond lengths [Å] and angles [deg]: Mo(1)−O(1) 1.730(4), Mo(1)−O(2) 1.738(4), Mo(1)−O(3) 1.685(5), Mo(1)−O(4) 1.852(5), O(4)−C(39) 1.343(10), Co(1)−O(1) 2.021(4), Co(1)−N(1) 2.315(5), Co(1)−N(2) 2.185(5), Co(1)−N(3) 2.269(5), Co(1)−S(1) 2.531(2), Co(1)−S(2) 2.512(2), Co(2)−O(2) 2.035(4), Co(2)−N(4) 2.306(5), Co(2)−N(5) 2.181(5), Co(2)−N(6) 2.313(5), Co(2)−S(1) 2.522(2), Co(2)−S(2) 2.482(2); O−Mo−O 106.5(2) [O(1)−Mo(1)−O(2)] to 111.7(2) [O(3)−Mo(1)−O(2)].

The normal potentials for **2** are slightly shifted to more negative potentials when compared with those of the acetato-bridged complex $[(L^{Me})Co^{II}_2(\mu\text{-OAc})]^+$ (**4**) ($E^1_{1/2} = 0.21$ V; $E^2_{1/2} = 0.60$ V).[14] These differences are likely a consequence of the charge differences. Recall that **2** is a neutral species whereas **4** is a monocation. It should be noted that the oxidized species are only stable on the time scale of a cyclic voltammetry experiment. All attempts to prepare these compounds by electrochemical or chemical oxidation led to unidentified decomposition products. Thus, while some of the above oxidations appear electrochemically reversible, they are all chemically irreversible.

**Description of Crystal Structures.** The X-ray crystal structures of complexes **2** and **3**·6MeOH were determined to establish the geometries about the metal ions as well as the bonding modes of the coligands. Experimental crystallographic data are summarized in Table 1. Further data are available in the Supporting Information.

**2·$CH_2Cl_2$.** The structure of **2**·$CH_2Cl_2$ consists of neutral complexes **2** and $CH_2Cl_2$ solvate molecules. There are no intermolecular interactions between the components. Figure 2 provides an ORTEP view of the structure of **2**.

The macrocycle adopts a bowl-shaped conformation, as observed in $[(L^{Me})_2Co^{II}_2(OAc)]^+$.[14] Each Co atom is coordinated by two S and three N atoms from the supporting ligand and an O atom of a $\mu_{1,3}$-bridging $MoO_4^{2-}$ ion in a severely distorted octahedral fashion. The distortions from the ideal octahedral geometry are manifested in the cis and trans L−Co−L bond angles, which deviate by as much as 24.9° from their ideal values. The Co−metal ligand bond lengths in **2** are very similar to those in **1**, indicative of a high-spin configuration for the $Co^{2+}$ ions.[28] The $MoO_4^{2-}$ unit is slightly tilted out of the $Co_2O_2$ plane, with the oxo atom O(3) pointing in the direction of one benzene ring [distance O(3)···centroid of phenyl ring = 3.612 Å]. The coordination about Mo is not perfectly tetrahedral. The mean Mo=O [1.712(7) Å] and Mo−O [1.761(6) Å] bond lengths differ by ca. 0.05 Å, and the O−Mo−O bond angles range from 106.3(3) to 111.5(3)°. Similar values have been observed for other molybdato-bridged complexes[29] and for the oxo−alkoxo compounds $MoO_2(OSiPh_3)_2$[9] and $MoO_2$(O-2,6-*t*-$Bu_2C_6H_2)_2$.[10] It is also worth mentioning that the Co−O distances in **2** [mean 1.988(6) Å] are shorter than those in **3** [2.027(4) Å], an effect that may be traced to stronger electrostatic coligand−metal interactions in **2**.

**3·6MeOH.** The crystal structure determination of **3**·6MeOH unambiguously confirmed the presence of a $\eta^2$-coordinated monomethyl orthomolybdate situated in the pocket of the $[(L^{Me})Co^{II}_2]^{2+}$ fragment (Figure 3). Further components are a centrosymmetric $[Mo_4O_{10}(OCH_3)_6]^{2-}$ counterion and MeOH solvate molecules. Note that the asymmetric unit contains only half of the atoms of the formula unit. The three independent MeOH molecules are H-bonded to each other (O···O = 2.81−2.87 Å). One of them is also H-bonded to the polymolybdate ion, but there are no H bonds with the $MoO_3(OMe)^-$ unit. The tilting of the latter toward the *t*-Bu group of the supporting ligand is indicative of an intramolecular van der Waals interaction [H(39a)···H(36b) = 2.313 Å].

The Mo−O distance to the methoxide ligand [1.852(5) Å] is significantly longer than the Mo=O distance [1.685(5) Å] to the terminal oxo function. The Mo−O distances to the bridging oxides (mean value 1.734 Å) lie between these two extreme values. This is in contrast to the free $MoO_3(OSiCPh_3)_3^-$ ion for which one long, one intermediate, and two short Mo−O distances have been reproted.[11] The bonding situation in the $MoO_3(OMe)^-$ ion may be described by the resonance structure depicted below, where bond orders of 2, 1.5, and 1 have been assigned to the individual M−O bonds.

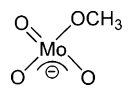


(29) Ghiladi, M.; McKenzie, C. J.; Meier, A.; Powell, A. K.; Ulstrup, J.; Wocadlo, S. *J. Chem. Soc., Dalton Trans.* **1997**, 4011−4018.

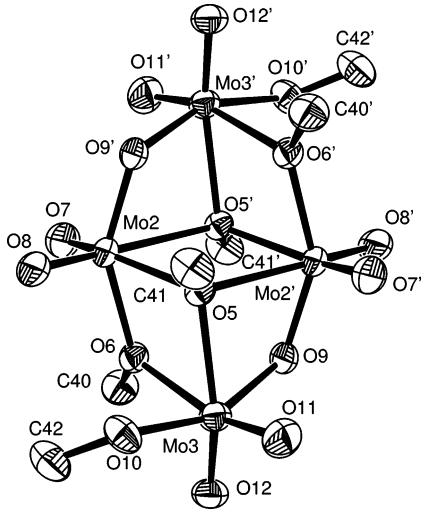


**Figure 4.** Structure of the $[Mo_4O_{10}(OCH_3)_6]^{2-}$ anion in crystals of **3**·$6CH_3OH$. Thermal ellipsoids are drawn at the 50% probability level. H atoms are omitted for reasons of clarity. Selected bond lengths [Å]: Mo(2)−O(5) 2.216(4), Mo(2)−O(6) 2.034(4), Mo(2)−O(5′) 2.390(4), Mo(2)−O(7) 1.691(4), Mo(2)−O(8) 1.691(4), Mo(2)−O(9′) 1.868(4), Mo(3)−O(5) 2.256(4), Mo(3)−O(6) 2.234(4), Mo(3)−O(9) 1.976(4), Mo(3)−O(10) 1.922(4), Mo(3)−O(11) 1.691(4), Mo(3)−O(12) 1.693(4). Symmetry code used to generate equivalent atoms: $-x, 2 - y, -z$.

It can be seen from Figure 3 that the centrosymmetric $[Mo_4O_{10}(OMe)_6]^{2-}$ counterion in **3** (Figure 4) is isostructural with that in $(MePPh_3)_2[Mo_4O_{10}(OCH_3)_6]$.[2] There are no unusual features as far as bond lengths and angles are concerned. The average Mo−($\mu$-O) [1.923(4) Å], Mo−$OCH_3$ [1.919(4) Å], Mo−($\mu$-$OCH_3$) [2.135(4) Å], Mo−($\mu_3$-$OCH_3$) [2.287(4) Å], and Mo−$O_t$ [1.692(4) Å] bond lengths are similar to the values of the compound above.[5]

## Conclusions

In summary, we have been able to trap a monomethyl orthomolybdate in the binding pocket of the $[(L^{Me})Co^{II}_2]^{2+}$ fragment. Work in progress is directed toward the synthesis of other ortho esters of the transition metals by taking advantage of the steric protection offered by the supporting ligand. These compounds may also exhibit novel reactivity features that are not seen for the free oxoanions.

**Acknowledgment.** Financial support from the Deutsche Forschungsgemeinschaft (Project KE 585/3-1,2,3) is gratefully acknowledged. We thank Prof. Dr. H. Vahrenkamp for providing facilities for X-ray crystallographic measurements.

**Supporting Information Available:** X-ray crystallographic data in CIF format. This material is available free of charge via the Internet at http://pubs.acs.org.

IC0603656